Available online at www.sciencedirect.com

Coordination Chemistry Reviews 242 (2003) 15–31

COORDINATION CHEMISTRY REVIEWS

www.elsevier.com/locate/ccr

Unusually structured organolanthanoid(III) dimers with two chiral, but not strictly equivalent, nitrogen-functionalized alkoxide bridges

Kathrin Schierwater [a], Hilka Hanika-Heidl [a], Marc Bollmann [a], R. Dieter Fischer [a,*], Robin K. Harris [b], David C. Apperley [b]

[a] *Institut für Anorganische und Angewandte Chemie der Universität Hamburg, Martin-Luther-King-Platz 6, 20146 Hamburg, Germany*
[b] *Department of Chemistry, University of Durham, South Road, Durham DH1 3LE, UK*

Received 23 October 2002; accepted 11 February 2003

Contents

Abstract

According to the crystallographic investigation of single crystals of four members of the chiral complex series $[Ln(\eta^5\text{-}C_5H_5)_2\text{-}\mu\text{-}(R)\text{-}(-)\text{-}OCH_2CH(Et)NMe_2]_2$ (Ln = Nd, Sm, Tb, Y)[1] the existence of dinuclear molecules with almost symmetrical $\{Ln_2(\mu\text{-}OCH_2)_2\}$ cores, but two notably different Ln–N separations ($\Delta(Ln{-}N) = 0.235{-}0.357$ Å) has been established. The formation of two non-equivalent $\{Ln(C_5H_5)_2OR\}$ fragments could independently be demonstrated by multinuclear (^{13}C, ^{15}N, ^{89}Y) CPMAS solid-state NMR studies of the complex with Ln = Y. In contrast, solution-state NMR spectra (^1H, ^{13}C, ^{89}Y) including, moreover, those of the homologues with Ln = La and Tm are consistent with virtually higher molecular symmetries (i.e. at least of C_2 symmetry) even at comparatively low temperatures. While, owing to the presence of chirogenic centres, the insight into structural details is improved, the overall molecular structure of the title complexes becomes slightly more complicated.

Keywords: Rare earths; Crystal structures; Solid-state NMR spectroscopy; Chirality; Alkoxide ligand

---

* Corresponding author. Tel.: +49-40-42838-3100/01; fax: +49-40-42838-2882.
E-mail address: fischer@chemie.uni-hamburg.de (R. Dieter Fischer).

[1] In the general formula $[Ln(C_5H_5)_2\text{-}\mu\text{-}(R)\text{-}(-)\text{-}OCH_2CH(Et)NMe_2]_2$, Ln = La (**1**), Pr (**2**), Nd (**3**), Sm (**4**), Tb (**5**), Y (**6**), Tm (**7**), Yb (**8**) and Lu (**9**). Me = methyl and Et = ethyl.

0010-8545/03/$ - see front matter © 2003 Elsevier B.V. All rights reserved.
doi:10.1016/S0010-8545(03)00025-0

1. Introduction

Metallocene complexes of the *tri*valent rare earth metals require always, in addition to two η^5-bonded cyclopentadienyl rings, one negatively charged ligand X, and unless X exhibits unusual steric congestion, these metallocenes tend to be (at least) dinuclear: $[Ln(C_5H_5)_2(\mu\text{-}X)]_2$. A chirogenic centre may thus reside either on the $\{Ln(C_5H_5)\}$ fragment (after suitable ring substitution), or on the bridging ligand X. Frequently, the latter option is easier to arrive at preparatively, and, moreover, helpful in various respects. (i) Particular (mainly cyclic) fragments of the ligand will adopt a favourite conformation (or configuration) which could easily be predicted. (ii) Eventually resulting prochiral atoms, or groups of atoms, can be detected in the NMR spectrum as pairs of diastereotopic resonance signals. (iii) When the Ln(III) ion is paramagnetic, not only the chemical shifts of ligand nuclei, but, moreover, the *separation* of the signals of prochiral groups is critically influenced (the separation being the more enlarged the closer the nuclei in question lie to the paramagnetic centre). (iv) When the chirogenic centre is separated from the paramagnetic Ln(III) ion by at most 3–4 chemical bonds, chiroptical phenomena (i.e. either circular dichroism or rotational dispersion) based upon f–f ligand field transitions of the lanthanoid ion may become observable.

One intrinsic difficulty that has generally to be faced in the field of rare earth complexes is the pronounced weakness of most metal-to-ligand bonds. Quite frequently, even a high-quality NMR spectrum of a dissolved complex may not reveal whether a distinct Ln–L bond persists statically, or is cleaved and re-established rapidly, unless in fortunate cases variable-temperature (VT) NMR studies will provide additional information. In the following, a series of homologous, alkoxide-bridged complexes $[Ln(C_5H_5)_2\text{-}\mu\text{-}OR^N]$ will be considered, the OR^N ligand of which involves one chiral carbon atom and one likewise coordinatively 'active' nitrogen atom. Although this particular atom turns out to be the only coordinatively labile one, the different impacts of the presence of chirogenic centres (of one singular configuration) turn out to cause a more complicated situation which is fully understood only by the concerted application of NMR spectroscopy and crystal structure analysis.

Recently, we have focused on, inter alia, the solution-state ^1H-NMR spectra of some mainly paramagnetic members of the chiral complex type $[LnCp'_2(R)\text{-}(-)\text{-}OCH_2C^*H(Et)NMe_2]_n$ (Ln = Pr, Nd, Sm, Yb, Lu; Cp′ = either C_5H_5 or, with Nd, C_5H_4Me; $n = 2$) [1]. Although rapid equilibria involving also mononuclear isomers (i.e. **C** and **D** of Scheme 1) could not strictly be ruled out [2], the appearance of signals indicating two equivalent Cp′ and N-bonded methyl groups at elevated temperatures, but two non-equivalent Cp′ and Me groups at lower temperatures, was ascribed to the dynamic interplay of the two *di*nuclear isomers **A** and **B**. The results of successful crystal structure analyses of closely related complexes like $[Yb(C_5H_4Me)_2(S)\text{-}(+)\text{-}OCH_2C^*H(Me)OMe]_2$ [3] and $[Yb(C_5H_5)_2OCH_2CH_2NR_2]_2$ (R = Me and Et) [4] have strongly supported the assumption of a dinuclear nature, at least in the solid-state.

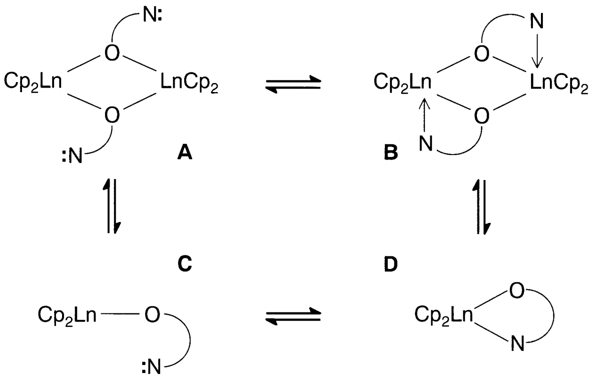

Scheme 1.

While the latter two achiral dimers were found to be strictly centrosymmetric [4], their chiral congeners are devoid of an inversion centre located halfway between the two metal atoms of **B**. Although, in principle, a twofold rotational axis perpendicular to the Ln_2O_2 fragment could persist, none of the relevant structure analyses of a chiral dimer has so far confirmed the presence of two strictly equivalent mononuclear units [3]. Yet, until now, all deviations from C_2 symmetry have turned out to be small enough to be correlated with minor perturbations like crystal packing effects rather than with significant variations in geometry between the two parts of the dimers. We now have succeeded in preparing single crystals suitable for crystallographic studies of members of the series $[Ln(C_5H_5)_2\text{-}(R)\text{-}(-)\text{-}OCH_2C^*H(Et)NMe_2]_2$ with Ln = Nd (**3**), Sm (**4**), Tb (**5**) and Y (**6**). These four homologues are in fact isostructural dimers, but of a notably modified, quite unexpected version of isomer **B** (Scheme 1), in that their two Ln–N distances differ constantly by at least 0.23 Å. This unusual crystallographic result is, moreover, supported and supplemented by a multinuclear (^{13}C, ^{15}N, ^{89}Y) CPMAS solid-state NMR study of **6**. On the other hand, RT/VT solution-state NMR studies (^1H, ^{13}C, ^{89}Y) of **1** (La), **3** (Nd), **4** (Sm), **5** (Tb), **6** (Y) and **7** (Tm) confirm the earlier reported [1] fluxionality of the complexes, which is continuously facilitated as the ionic radius of Ln^{3+} decreases, leading at sufficiently high temperatures even to virtually centrosymmetric molecules.

As this contribution differs from a conventional review article, an Epilogue is added in order to clarify briefly how the subject presented in the main part is embedded both chronologically and in view of its actual stage of development into the field of functionalized (and chiral) bis(cyclopentadienyl)lanthanoid(III) alkoxides.

2. Synthesis and general properties of 1–7

All complexes of the type [LnCp$'_2$-(*R*)-(−)-$OCH_2CH(Et)NMe_2$]$_2$, including the so far unreported homologues **1**, **3**, **5**, **6** and **7** with Cp′ = C_5H_5 only and Ln = La, Nd, Tb, Y and Tm, respectively, were prepared as described previously [1] by reacting equimolar quantities of [Ln(C_5H_5)$_3$] and (*R*)-(−)-2-dimethylaminobutanol in toluene solution, starting always at low temperature. Fractions of the toluene solutions, assumed to contain the final product together with cyclopentadiene (1:1), were further concentrated and used for crystal growth experiments. Generally, small quantities of *n*-hexane were added carefully to these solutions. The single crystals resulting usually after few days at room temperature were long, initial transparent needles that tended to get a slurry-like surface after more than 1 week.

Base-free [Y(C_5H_5)$_3$] was also reacted with racemic 2-dimethylaminobutanol in the expectation of obtaining a mixture of the (*R*,*R*)-, (*S*,*S*)- and (*R*,*S*)-diastereomers of **6**. According to the NMR spectra of the dissolved product (vide infra), signals of the (*R*,*S*)- (or *meso*) form could in fact be observed, too, which observation may be considered as the first confirmation of the presence of *di*nuclear species also in solution. Polycrystalline **5** and **7** (Tb and Tm) were subjected to fast-atom bombardment (FAB) mass spectrometric studies. In both cases, the *m*/*e* value of the most intense fragment (745.6 and 765.6, respectively) can be unambiguously assigned to a *di*nuclear molecular ion without just one of its initially present C_5H_5 units. Surprisingly, solid samples (single crystals even better than bulk material) seem to survive a short exposure to air (of ≤1 min) which feature turned out to be helpful for the preparation of samples for successful X-ray powder diffractometric and solid-state NMR studies of **6**.

The O→Ln bonds tying together two mononuclear fragments (**D**) in the isomers **A** or **B** (see Scheme 1) seem to be remarkably strong, since the room temperature ^{1}H-NMR spectra of solutions containing both **1** and **3**, and **1** and **4** (1:1 in CD_2Cl_2), respectively, displayed, even after several hours, just the superposition of the individual spectra of the two intermixed *homo*dinuclear homologues. Any significant tendency to undergo metathetical rearrangements (involving also *hetero*dinuclear species) would undoubtedly have led to notable changes in the general appearance of the resulting spectra. A spectrum displaying clearly the resonances of **1**, **3** *and* of the expected heterodinuclear derivative was, on the other hand, observed when a mixture of [La(C_5H_5)$_3$] and [Nd(C_5H_5)$_3$] (1:1) was reacted with (*R*)-(−)-dimethylaminobutanol [5].

3. Crystal structure analyses of 3–6

Crystal data, together with details of data collection and refinement, for four different complexes (**3**–**6**) are listed in Table 1. The result of a room temperature study of another crystal of **5** (Ln = Tb) is also included in order to investigate if the non-equivalence of the two Ln···N interactions is temperature-dependent. All five crystals are isostructural and contain oxygen-bridged dimers. As expected, the configuration of the chiral β-carbon atoms of the alkoxide ligands is the same as in (*R*)-(−)-2-dimethylaminobutanol. The central Ln_2O_2 fragments are planar throughout. However, in contrast to all solution-state NMR results (vide infra), each dimer involves two non-equivalent mononuclear building blocks. Most pronounced differences are reflected for the two Ln–N distances, while the central {Ln_2(μ-OCH_2)$_2$} fragments and the metal-to-C_5H_5 distances are comparatively weakly affected (Table 2). On the other hand, the two puckered five-membered metallacycles that are fused together via two Ln–O bonds are not strictly superimposable (although they are no reciprocal enantiomers). In consequence, the Ln(1)···C and Ln(2)···C separations of **4** and **6**, respectively, involving the four nitrogen-bonded methyl carbon atoms differ considerably, too.

In Fig. 1, the ORTEP plot of one molecule of **6** (Ln = Y) is shown as an exemplar for all other crystallographically investigated homologues, choosing here a perspective perpendicular to the Y_2O_2 plane. Fig. 2 presents, for comparison, a view along the Y_2O_2 plane. The latter perspective also indicates that the two C(11)–C(12) and C(21)–C(22) vectors enclose very different angles with the vectors Ln1–O1 and Ln2–O2, respectively (see Table 2). In spite of the usually quite long Ln–N distances as found for **3**–**6**, all of the structurally investigated complexes are likely to involve *two* distinct, clearly non-equivalent, Ln–N interactions. For comparison, several other organolanthanoid complexes with potential or real Ln–N interactions are listed in Table 3. Thus, two nitrogen atoms of the mononuclear complex [La{$C_5H_4(CH_2)_2NMe_2$}$_3$] (**10**) may be considered to occupy the axial positions of a (distorted) trigonal bipyramid (with three equatorial C_5 centres). Although one La–N distance is undoubtedly very long (3.688 Å, see Table 3), it seems suggestive to associate that particular configuration with two non-equivalent Ln···N 'contacts' [6b]. In contrast, the neodymium homologue [Nd{$C_5H_4(CH_2)_2NMe_2$}$_3$] (**11**) of **10** displays only one Nd–N interaction, most probably

Table 1
Selected crystallographic data for **3**–**6**

Compound	**3**	**4**	**5** [a]	**5**	**6**
Empirical formula	$C_{32}H_{48}N_2Nd_2O_2$	$C_{32}H_{48}N_2O_2Sm_2$	$C_{32}H_{48}N_2O_2Tb_2$	$C_{32}H_{48}N_2O_2Tb_2$	$C_{32}H_{48}N_2O_2Y_2$
Formula weight	781.20	793.42	810.56	810.56	670.54
Temperature (K)	153(2)	153(2)	293(2)	153(2)	153(2)
Crystal system	Orthorhombic	Orthorhombic	Orthorhombic	Orthorhombic	Orthorhombic
Space group	$P2_12_12_1$	$P2_12_12_1$	$P2_12_12_1$	$P2_12_12_1$	$P2_12_12_1$
a (Å)	8.569(13)	8.5244(11)	8.5613(17)	8.6101(17)	8.4997(4)
b (Å)	11.349(11)	11.2732(15)	11.458(2)	11.372(2)	11.3340(6)
c (Å)	32.77(3)	32.439(4)	32.727(7)	32.468(7)	32.2252(16)
V (Å^3)	3187(7)	3117.3(7)	3210.5(11)	3179.1(11)	3104.4(3)
Z	4	4	4	4	4
ρ_{calc} (g cm^{-3})	1.628	1.691	1.677	1.694	1.435
μ (mm^{-1})	3.251	3.760	4.398	4.442	3.750
$F(000)$	1560	1576	1600	1600	1392
Θ Range (°)	2.46–26.55	1.91–30.06	2.46–27.56	2.45–25.07	2.20–30.00
Total reflections	5098	79 816	5482	5390	75 940
Unique reflections	4578	9099	5047	4495	9027
Refinement parameter	350	349	350	350 [c]	350
Extinction coefficient	0.00025(15)	0.0	0.00089(9)	0.0026(3)	0.00139(16)
R_{int}	0.0714	0.0646	0.0339	0.1168	0.1420
R_1 [b]	0.0576	0.0263	0.0364	0.0525	0.0374
wR_2 [b]	0.1180	0.0523	0.0696	0.1271	0.0639
R_1 (all data)	0.0978	0.0287	0.0548	0.0732	0.0925
wR_2 (all data)	0.1396	0.0528	0.0771	0.1458	0.0699
Goodness-of-fit for F^2	1.066	1.046	1.075	1.054	0.794
Flack parameters/esd	−0.0822/0.562	−0.0218/0.0101	−0.0165/0.0256	0.0062/0.00448	−0.0203/0.0054
Largest difference peak and hole (e Å^{-3})	1.323 and −1.484	0.989 and −0.794	0.734 and −0.640	1.465 and −1.630	0.609 and −0.913

[a] Room temperature study.
[b] For $I \geq 2\sigma(I)$.
[c] With 24 restraints (otherwise zero).

because the standard radius of the Nd^{3+} ion is smaller than that of La^{3+} [6a]. The Nd–N distance of **11** (Table 3) matches with the shorter of the two Nd–N separations of **3** (Table 2). In principle, the acceptance of the very long La–N distance of **10** as still 'coordinative' appears to be rather delicate, but it would obviously imply the acceptance of the longer Nd–N distance of **3** as 'coordinative', too. The presently longest La–N 'bond' in the Cambridge database is associated with a distance of 3.028 Å only. The averaged Nd–N distance of **3** (2.827 Å) exceeds only slightly the corresponding average of the mononuclear complex **13** (2.788 Å). Interestingly, for none of the complexes **3**–**6** do the atoms of the alkoxide ligand with the more remote (from Ln) N atom display significantly larger thermal ellipsoids, as might be likely for otherwise non-anchored molecular groups. A more convincing argument against the assumption of only one really metal-coordinated N atom in the binuclear title complexes results from the solid-state NMR study of complex **6**, according to which the chemical shifts of the two observable signals (of either the ^{15}N- or ^{89}Y nuclei) do not differ significantly (vide infra).

While the Ln···Ln separations, the Ln–C distances and the averaged Ln–O distances of the title complexes decrease as usual along with the effective radius of the metal ion, the averaged Ln–N distance varies between 2.815 (Sm) and 2.861 Å (Tb, Y). Two almost equal Sm–N distances (of ca. 2.835 Å, close to the averaged value of **4**) were found for the dinuclear, and practically C_2-symmetrical complex **12** (Table 3), however, the Sm_2O_2 fragment of **12** is significantly folded along O1···O2 [1]. The unsymmetrical, dinuclear complex **21** displays notably shorter Sm–N distances than **4** and **12**. Finally, it is noted that the Ln···Ln distance turns out to be significantly expanded whenever the nitrogen atoms belonging to the alkoxide bridge are also Ln-coordinated (compare e.g. the Ln···Ln distances of the pairs of complexes: **23/3**, **17/4** and **22/14**, respectively, of Tables 2 and 3).

Interestingly, also the two centrosymmetric dimers **14** and **15** (Table 3) are reported to display rather long Yb–N distances of 2.691 and 2.895 Å, respectively. The latter value, which is likely to reflect more pronounced steric Et···C_5H_5 congestion (affecting only one of the two C_5H_5 ligands), even exceeds slightly the averaged Y–N distance of the chiral complex **6**. The shorter of the two Y–N distances of **6** is still longer (by 0.183 Å) than the Y–N distance in the chiral mononuclear complex [$\{C_5Me_4SiMe_2C_5H_3(CH_2)_2NMe_2\}YCl$] [16], wherein the total hapticity is, on the other hand, lower than in **6**. The difference Δ of the two Ln–N distances of **3**–**6** varies

Table 2
Selected interatomic distances (Å) and angles (°) for **3**–**6** [a]

	3 (Nd)	**4** (Sm)	**5** (Tb,RT)	**5** (Tb)	**6** (Y)
Bond distances					
Ln1–cent 1	2.5536(10)	2.5062(2)	2.4740(4)	2.4984(7)	2.4582(4)
Ln1–cent 2	2.5254(10)	2.4940(2)	2.4801(4)	2.4839(8)	2.4505(3)
Ln2–cent 3	2.5302(10)	2.4834(2)	2.4546(4)	2.4634(8)	2.4218(3)
Ln2–cent 4	2.5346(10)	2.4804(1)	2.4431(4)	2.4630(7)	2.4230(3)
Ln1–O1	2.353(11)	2.307(2)	2.280(6)	2.312(10)	2.257(2)
Ln1–O2	2.330(11)	2.311(2)	2.306(7)	2.309(10)	2.283(2)
Ln2–O1	2.355(11)	2.328(2)	2.290(7)	2.312(10)	2.274(2)
Ln2–O2	2.306(11)	2.260(2)	2.245(6)	2.271(10)	2.206(2)
Ln1–N1	2.710(16)	2.687(3)	2.695(10)	2.703(13)	2.685(3)
Ln2–N2	2.945(17)	2.944(3)	3.027(10)	3.018(14)	3.038(3)
Ln1···Ln2	3.863(6)	3.8004(6)	3.7535(10)	3.7710(13)	3.7012(5)
Ln1···C15	3.54(2)	3.553(4)	3.573(13)	3.540(18)	3.563(4)
Ln1···C16	3.54(2)	3.517(4)	3.549(12)	3.58(2)	3.519(4)
Ln2···C25	3.872(19)	3.660(4)	3.975(14)	3.751(17)	3.785(4)
Ln2···C26	3.64(2)	3.877(4)	3.774(13)	3.995(18)	3.987(4)
Bond angles					
cent1–Ln1–cent2	122.5(0.91)	122.6(0.15)	122.1(0.45)	122.8(0.75)	122.7(0.16)
cent3–Ln2–cent4	123.6(0.88)	123.5(0.15)	124.2(0.44)	124.4(0.72)	124.3(0.15)
O1–Ln1–O2	68.2(4)	68.39(7)	68.8(2)	69.6(4)	69.14(8)
O1–Ln2–O2	68.6(4)	68.88(2)	69.6(2)	70.2(4)	70.19(8)
O1–Ln1–N1	66.8(4)	66.75(7)	67.1(3)	66.6(4)	67.39(9)
O2–Ln2–N2	65.5(4)	65.49(9)	64.5(3)	64.6(4)	64.67(9)
Ln1–O1–Ln2	110.3(4)	110.15(8)	110.4(2)	109.3(4)	109.54(10)
Ln1–O2–Ln2	112.9(4)	112.52(9)	111.1(2)	110.9(4)	111.08(10)
Dihedral angle 1 [b]	7(2)	7.3(4)	9.3(12)	4.3(18)	8.8(4)
Dihedral angle 2 [c]	46(2)	48.7(3)	51.8(11)	54(2)	49.9(4)

[a] Data collection at 153 K except for **5**(RT).

[b] Of the two vectors Ln1–O1 and C11–C12.

[c] Of the two vectors Ln2–O2 and C21–C22.

between 0.235 (Nd) and 0.335±0.02 Å (Sm, Tb, Y), which Δ-values turn out to exceed drastically that reported [12] for the likewise chiral complex **20** (0.082 Å), wherein the two $\{Ln(C_5H_5)_2\}$ fragments are substituted by notably smaller $\{GaMe_2\}$ units. For comparison, the difference found for the organogallium dimer **20** still exceeds the corresponding Δ-value of the two coordinative $O(Me) \rightarrow Ln$ interactions in the chiral congener $[Yb(C_5H_4CH_3)_2$-μ-(*S*)-(+)-$OCH_2CH(Ph)$-$OMe]_2$ [3] of **3**–**6** ($\Delta = 0.037$ Å).

4. Solid-state NMR study of 6

According to a comparison of the experimental X-ray powder diffractogram (XRPD) of **6** with the simulated one based upon data from the single-crystal X-ray study (see Fig. 3), polycrystalline ('bulk') **6** retains the structure known from the single-crystal structure analysis. Therefore, the diamagnetic complex **6**, which contains, (apart from the nuclei ^{13}C and ^{15}N), metal ions with the spin-1/2 nucleus ^{89}Y (100% abundance), turned out to be a promising solid-state NMR candidate.

Actually, both the ^{89}Y and the ^{15}N spectra of **6** displayed two distinct singlets (Fig. 4) which observation is consistent with the existence of two non-equivalent $\{Y(C_5H_5)_2OCH_2CH(Et)NMe_2\}$ fragments. The two ^{89}Y lines clearly reflect metal centres of slightly different coordinative saturation, the signal at lower frequency belonging presumably to the somewhat 'more tightly' coordinated yttrium ion. Even in a slow-spinning experiment (<500 Hz) of **6** only one sideband for each signal could be generated, suggesting for both yttrium centres a 'high' degree of symmetry. Ignoring the use of slightly different reference samples for the present study ($Y(NO_3)_3/H_2O$) and for an earlier ^{89}Y solution-state (THF) study (YCl_3/H_2O) [17], the chemical shifts of **6** are found to range between those of $[Y(C_5H_4Me)_2(\mu\text{-}H) \cdot THF]_2$ (−92 ppm) and $[Y(C_5Me_5)_2(\mu\text{-}Cl)_2K(THF)_2]$ (−324 ppm). Surprisingly, $[Y(C_5H_4Me)_2(\mu\text{-}Me) \cdot THF]_2$ is reported to resonate at +40 ppm.

While in the ^{89}Y spectrum no multiplets are expected, the ^{15}N resonances might, in principle, give rise to two doublets owing to (^{89}Y,^{15}N) coupling. Although a recent solid-state ^{171}Yb-NMR study of a diamagnetic organoytterbium(II) complex has led to a $|^{1}J(^{171}Yb,^{31}P)|$ value

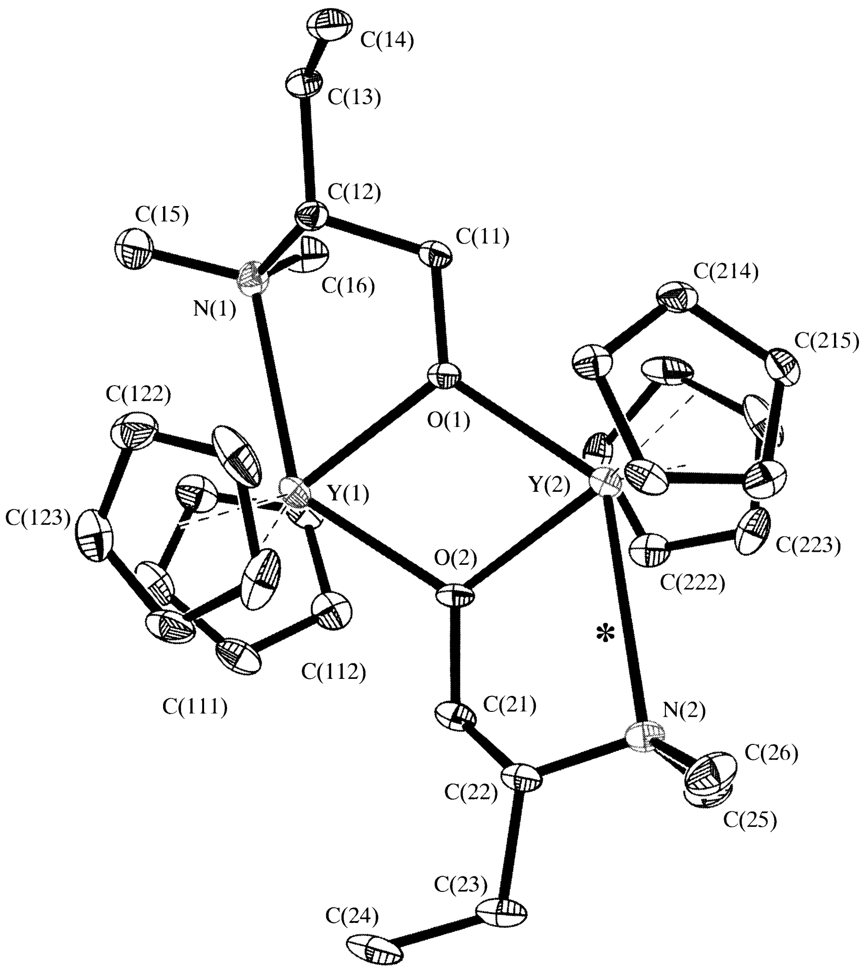

Fig. 1. Molecular structure of **6**, viewed perpendicular to the planar Y_2O_2 core. The asterisk denotes the longer of the two N–Y distances.

of 804 Hz [18], the largest reported $|^1J(^{89}Y,^{13}C)|$ values amount to 50 Hz [19]. Corresponding $|^1J(^{89}Y,^1H)|$ values hardly exceed 27 Hz [20]. We are therefore reluctant to ascribe the two observable ^{15}N lines of **6** to a spin doublet (with $|^1J(^{89}Y,^{15}N)|$ of ca. 125 Hz), inasmuch as strict equivalence of the two N atoms of the dimer should then be implied, in clear contrast to the ^{89}Y-NMR result. The assumption of notably weaker

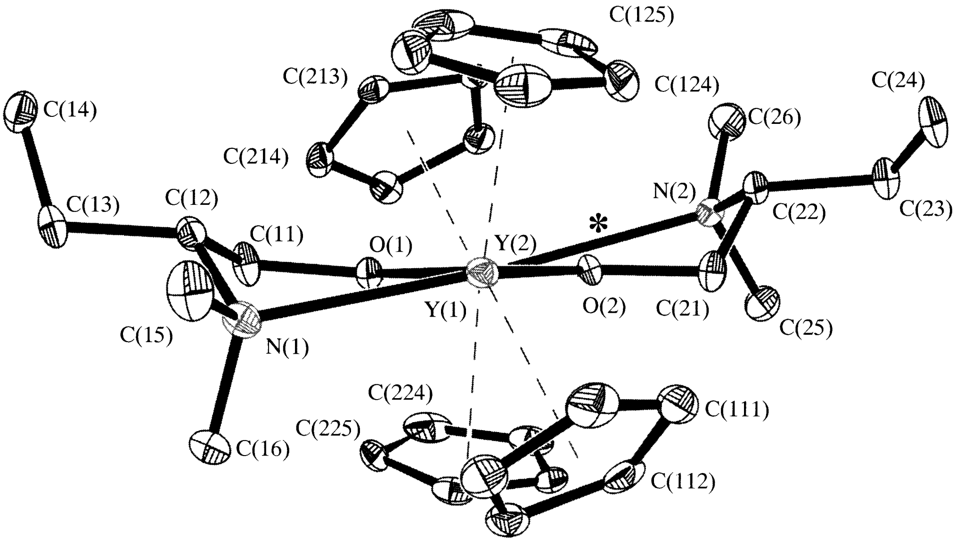

Fig. 2. Molecular structure of **6**, viewed along the Y(1)···Y(2) axis. The asterisk denotes the longer of the two N–Y distances.

Table 3
M–N, M···M′ and (occasionally)[a] M–O distances of selected complexes from the literature

Compound	No.	Reference	d(M–N) or d(M–O) (Å)	d(M···M′) (Å)
$[La\{C_5H_4(CH_2)_2NMe_2\}_3]$ [b]	**10**	[6a]	2.898(6) and 3.688(5)	–
$[Nd\{C_5H_4(CH_2)_2NMe_2\}_3]$ [c]	**11**	[6a]	2.70(1), 2.73(1)	–
$[Sm(C_5H_5)_2\{\mu\text{-}(R)\text{-}OCH(Ph)CH_2NMeBz\}]_2$	**12**	[1]	2.834(12) and 2.837(11)	3.935(5)
$[Nd\{C_5H_4(CH_2)_2NMe_2\}_2Cl]$ [b]	**13**	[7]	2.772(2) and 2.804(2)	–
$[Yb(C_5H_5)_2\{\mu\text{-}O(CH_2)_2NMe_2\}]_2$	**14**	[4]	2.691(4)	3.7072(6)
$[Yb(C_5H_5)_2\{\mu\text{-}O(CH_2)_2NEt_2\}]_2 \cdot THF$	**15**	[4]	2.895(7)	3.6910(8)
$[Lu(C_5H_5)_2(CH_2)_3NMe_2]$	**16**	[8]	2.37(1)	–
$[Sm(C_5H_5)_2\{\mu\text{-}OC_{10}H_{19}\}]_2$ [d]	**17**	[9]	2.290(5)–2.365(5)	3.648(15)
$[Nd(C_5H_5)_3(NCMe)_2]$	**18**	[10]	2.764(5)	–
$[Nd\{OC(CMe_3)_3\}_3(NCMe)_2]$ [e]	**19**	[11]	2.641(7) and 2.627(7)	–
$[GaMe_2\{\mu\text{-}(S)\text{-}OCH_2CH(R)NMe_2\}]_2$ [f]	**20**	[12]	2.400(3) and 2.482(3)	3.161(1)
$[Sm\{C_5H_4(CH_2)_2OMe\}\{(1,2\text{-}OC_6H_4CHN)_2\text{-}1,2\text{-}C_6H_{10}\}]_2$ [g]	**21**	[13]	2.254(4), 2.527(5), 2.561(5), 2.680(4)	3.8037(7)
$[Yb(C_5H_5)_2\text{-}\mu\text{-}OR]_2$ [h]	**22**	[14]	2.17(1), 2.19(1)	3.483(3)
$[Nd(C_5H_4CMe_3)_2(\mu\text{-}OH)]_2$	**23**	[15]	2.252(4), 2.262(3)	3.615(4)

[a] In the absence of Ln–N bonds only.
[b] Two Ln–N interactions per molecule.
[c] With only one distinct Ln–N interaction per molecule, but two different molecules per unit cell.
[d] $OC_{10}H_{19}$ = *iso*-mentholate.
[e] Nd–N distances only.
[f] R = *i*-C_3H_7.
[g] Sm–N distances only.
[h] R = $(CH_2)_4Me$.

(^{89}Y,^{15}N)-coupling constants than the half width of the observed lines seems to be more realistic. The chemical shift values of the two ^{15}N singlets are very similar supporting the view (vide supra) that both nitrogen atoms should be considered as metal-coordinated.

In the ^{13}C spectrum of solid **6** the most obvious evidence in favour of two non-equivalent building blocks is the appearance of four *N*-methyl resonances at 37.7, 41.4, 44.8 and 46.9 ppm (section A of Fig. 5). All four signals seem to be accompanied by a high-frequency shoulder which might arise through second-order interaction with an adjacent quadrupolar ^{14}N nucleus [21]. The four signals were retained in a dipolar dephasing experiment, as were the two signals at 13.3 and 16.9 ppm (section D) which presumably belong to the methyl carbon atoms of the two non-equivalent ethyl groups. The four singlets between 65 and 75 ppm (section B) can be ascribed to the two pairs of α-CH_2

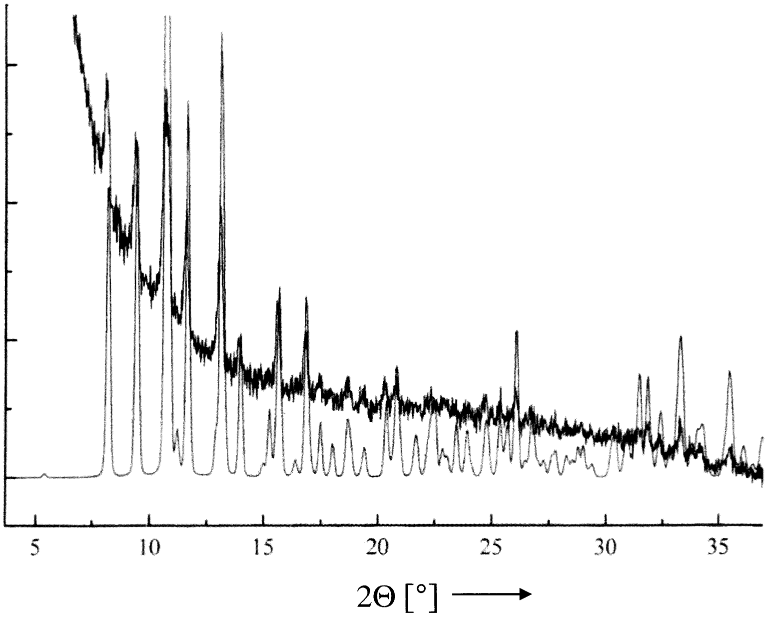

Fig. 3. Comparison of the experimental (top) with the simulated (bottom) powder X-ray diffractogram of **6**.

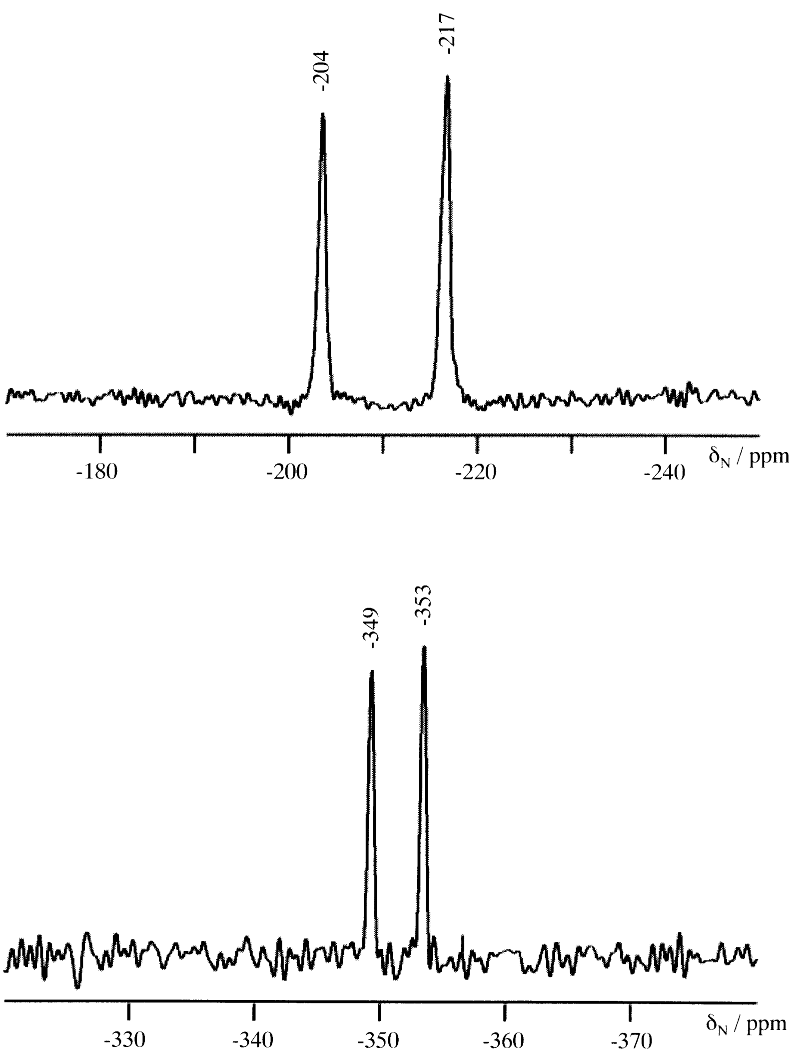

Fig. 4. CPMAS solid-state NMR spectra of the nuclei Y-89 (top) and N-15 (bottom) of **6**.

and β-CH fragments of the two non-equivalent metallacyclic rings (see Fig. 1). Optimal resolution of the intense resonances between 109 and 111 ppm (section C of Fig. 5) leads to a triplet-like signal. Since four different, still rapidly (on the NMR timescale) rotating C_5H_5 ligands are expected, it seems reasonable to consider the most intense, central line of the quasi-triplet as due to the overlap of two very close-lying individual lines. Interestingly, according to an early solid-state ^{13}C-NMR study of the unsymmetrical complex $[Lu(C_5Me_5)_2(\mu\text{-}Me)Lu(Me)(C_5Me_5)_2]$, which also involves four different C_5Me_5 ligands, four ring carbon signals (between 114.4 and 120.6 ppm) but only three (ring) methyl carbon signals were observable [19]. Although, somewhat surprisingly, not all the signals for the carbon atoms of the ethyl units of solid **6** could safely be located in spite of several changes of the spin rate, the solid-state NMR results of this sample in total provide convincing evidence for the presence of two significantly non-equivalent $\{Y(C_5H_5)_2OCH_2CH(Et)NMe_2\}$ fragments in one molecule.

5. NMR spectroscopy of the dissolved complexes

The room temperature solution-state (CD_2Cl_2) ^{1}H-NMR spectra of all complexes of the type $[Ln(C_5H_5)_2\text{-}(R)\text{-}(-)\text{-}OCH_2CH(Et)NMe_2]_2$ display either one ($Int_{rel} = 10$) or two equally intense ($Int_{rel} = 5$) singlet(s) for the C_5H_5 ring protons, either one ($Int_{rel} = 6$) or two ($Int_{rel} = 3$) singlet(s) for the N-bonded methyl groups, another singlet (or unresolved triplet) with $Int_{rel} = 3$ for the CH_3 fragment of the ethyl group, and a total of five singlets (or multiplets) with $Int_{rel} = 1$ each. The last-mentioned five signals should belong to the two prochiral methylene groups (in the α- and γ-position) and to the β-methine proton of the alkoxide ligand [1]. The spectral patterns of the dissolved complexes thus do not match with the solid-state NMR results for **6** (vide supra), no matter whether at room temperature only eight (heavier Ln's) or ten signals (lighter Ln's) appear. The solution-state spectra rather suggest the presence either of monomers or of virtually centrosymmetric dimers, owing to rapid fluxionality.

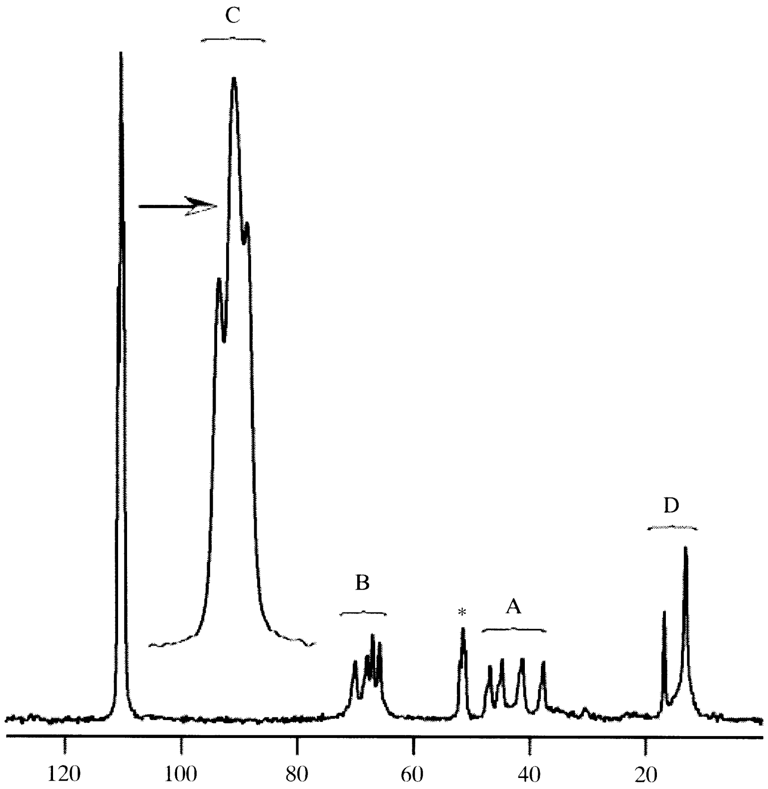

Fig. 5. Carbon-13 solid-state NMR spectrum of **6** (a residual side band is depicted by an asterisk).

Usually the C_5H_5 and $(N)Me_2$ protons could be readily identified owing to their characteristic relative intensities. To illustrate the occasional difficulties in also assigning appropriately the five equally intense resonances with $Int_{rel} = 1$, the experimental data for several homologues (i.e. with diamagnetic, moderately paramagnetic and strongly paramagnetic metal ions) are listed in Table 4. While the assignments for Ln = La and Y are well supported by the appearance of characteristic multiplet features which strongly resemble those already discussed for **9** (Ln = Lu [1]; see also Fig. 6b), that for Ln = Nd is based on successful $^1H/^1H$- and $^1H/^{13}C$ COSY correlation studies [22]. At room temperature, the resonance of the diastereotopic γ-methylene protons of **3** must be considered as accidentally degenerate; at higher temperatures clearly two singlets appear. Usually, the diastereotopic splitting of the $\gamma\text{-}CH_2$ resonances turns out to be weaker than that of the $\alpha\text{-}CH_2$ resonances because this group is more remote from the paramagnetic centre(s) [1]. In view of the compara-

Table 4
Solution-state ^{1}H-NMR data of protons occupying α-, β- and γ-positions (solvent: CD_2Cl_2)

Ln/No.	$\alpha\text{-}CH_2$		β-CH	$\gamma\text{-}CH_2$		Reference
La (**1**)	4.05dd [a]	3.75t [b]	2.82m	1.65m [c]	1.07	
Pr (**2**)	−6.66s	−13.47s	−0.32m	−10.07m	−12.71m	[1]
Nd (**3**)	−5.63s,br	−3.09s,br	−12.12s,br	−8.05s [d]		
Sm (**4**)	−1.52t,br	−2.03t [e]	Not observed [f]	−0.50m	−1.00m	[1]
Tb (**5**)	−152	−207	−267s	−118.4s [g]	−119.6s [g]	
Y (**6**)	3.85dd	3.53t	2.91m	1.66m	1.04 [c]	
Tm (**7**)	163	144s	117s	70s	66s	
Yb (**8**)	77.94s	67.42s	71.0	39.61s	33.37s	[1]

[a] $J = 11.86$ and 4.78 Hz.

[b] $J = 11.02$ Hz.

[c] Partial overlap with the resonances of the $\delta\text{-}CH_3$ protons.

[d] $I_{rel} = 2$.

[e] $^3J = 10$ Hz.

[f] In toluene-d_8, one additional doublet centred at −1.99 ppm appears.

[g] Comparatively sharp signal.

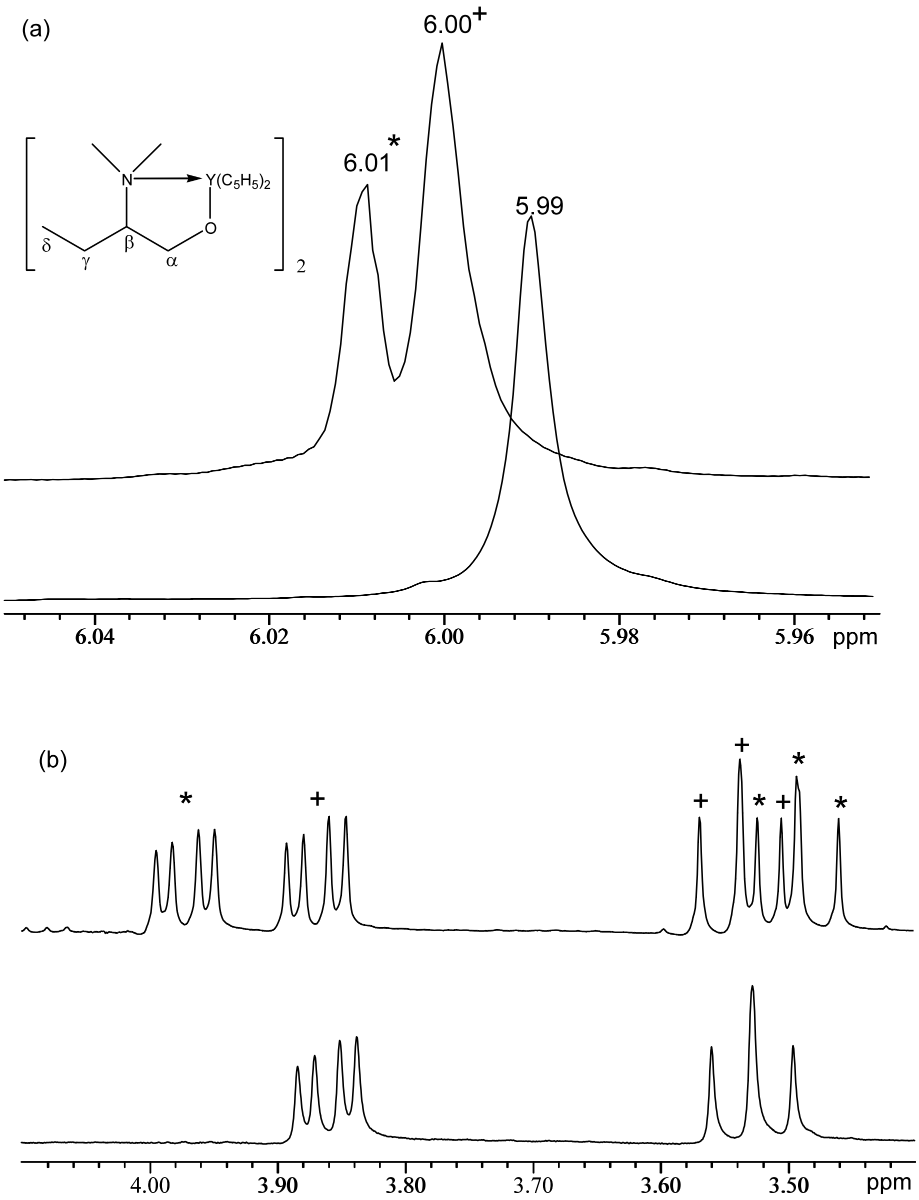

Fig. 6. (a) C_5H_5 proton resonance(s) of pure **6** (bottom) and a mixture of racemic (+) and *meso*-configured (*) **6** (top). Solvent: CD_2Cl_2. (b) Comparison of the proton resonances of the α-CH_2 fragments of pure **6** (bottom) with those of a mixture of racemic (+) and *meso*-configured (*) **6** (top). Solvent: CD_2Cl_2.

tively weak influence of the paramagnetism of the Sm^{3+} ion on the NMR spectra, the spectral data of complex **4** follow closely those of the diamagnetic homologues. The corresponding five, equally intense, singlets of the Yb complex could reliably be identified after a complete VT NMR study (vide infra).

Carbon-13 shifts of five homologues are collected in Table 5. The numbers of observed signals again agree with those expected for virtually centrosymmetric, fluxional molecules (e.g. either eight for type **B** of Scheme 1 or six for the fluxional type **A**). While the eight signals of the paramagnetic complex **2** (Ln = Pr; $\delta = 198.0$, 117.3, 8.6, 7.2, −30.0 w,br and −38.0 w,br ppm) cannot be assigned yet, those of the Nd homologue **3** may be ascribed to distinct carbon atoms by a two-dimensional $^1H/^{13}C$-correlation (at 500 MHz) [22]. Again, the shifts of the ring carbon atoms of **4** (Ln = Sm) are not strongly affected by the paramagnetism of the adjacent metal ion, whereas the isotropic shifts of **3** clearly reflect the paramagnetism of the Nd^{3+} ion. Interestingly, the sign of the isotropic ^{13}C shift of **3** changes three times between the C_5H_5 and the nitrogen-bonded methyl carbon atoms. The weak, but still non-negligible, influence of the two paramagnetic Sm^{3+} ions on the shifts of the ^{13}C nuclei of complex **4** might raise the following question: as the coalescence temperature T_c of the methyl protons of the NMe_2 group of **4** is known to lie notably above room temperature (vide

Table 5
Room temperature ^{13}C shifts (ppm) for **1**, **3**, **4**, **6** and **9**, dissolved in CD_2Cl_2

Ln/No.	C_5H_5	$(CH_3)_2$	α-CH_2	β-CH	γ-CH_2	δ-CH_3	Reference
La (**1**)	112.35	44.71	69.34	68.79	14.22	13.00	
	112.16	37.93					
Nd (**3**)	182.60	−10.82 [a]	−25.00	25.39	10.64	8.30	
	146.84	−16.30 [b]					
Sm (**4**)	106.3	44.6	76.8	67.2	37.6 [c]	11.4	[1]
	105.1						
Y (**6**)	109.74 [d]	Absent	68.51	67.76	14.53	12.99	
Lu (**9**)	109.27	42.56	68.34	67.60	14.75	13.02	[1]

[a] Correlates with ^{1}H resonance at −15.50 ppm.
[b] Correlates with ^{1}H resonance at −15.95 ppm.
[c] For an alternative assignment, see the text.
[d] Resonance of the *meso*-form, dissolved together with racemic **6**.

infra), *two* NMe_2 ^{13}C resonances might be expected, too. Thus, the signal at 37.6 ppm, which was first ascribed to the γ-CH_2 group [1], could alternatively be considered as the second resonance of the NMe_2 group. Then, however, the γ-CH_2 signal would be absent. On the other hand, the solution-state ^{13}C spectra of **6** (both in CD_2Cl_2 and in THF-d_8) did not display the resonance(s) of the nitrogen-bonded methyl groups, which appear clearly in the solid-state ^{13}C-NMR spectrum between 37.7 and 46.9 ppm (vide supra). The CD_2Cl_2 spectrum just seems to indicate a very faint and broad double hump between 40 and 50 ppm, suggesting arrival at the corresponding coalescence temperature. Interestingly, the chiral complex $[\{C_5Me_4SiMe_2C_5H_3(CH_2)_2NMe_2\}YCl]$ (vide supra) is reported to display only one distinct NMe_2 ^{13}C resonance at 45.57 ppm [16]. In view of the facile observability of the γ-CH_2 and δ-CH_3 ^{13}C resonances in the solution-state spectra, the two ^{13}C resonances of solid **6** at 13.3 and 16.9 ppm might alternatively be ascribed to the carbon atoms of two virtually equivalent ethyl groups.

The reaction product of $[Y(C_5H_5)_3]$ and racemic 2-dimethylaminobutanol gave rise to solution-state NMR spectra typical of a mixture of the dinuclear racemic (i.e. (*R*,*R*) and (*S*,*S*)) and *meso* (*R*,*S*) configured diastereomers of **6**. Thus, the ^{1}H-NMR spectrum displays, inter alia, two C_5H_5 resonances (Fig. 6a) and a complete doubling of all of the multiplets due to the α-methylene protons of the five-membered metallacycle (Fig. 6b). Interestingly, the signals of the racemate appeared very weakly, but reproducibly, displaced from the positions observed for enantiomerically pure **6**, suggesting some faint intermolecular interaction. Moreover, the C_5H_5 proton resonance of the *meso* form could occasionally be resolved to a doublet, corresponding to a ^{89}Y, ^{1}H coupling constant of ca. 1.1 Hz. The ^{13}C spectrum of the *rac*/*meso*-mixture displays two close-lying C_5H_5 carbon signals, whereas the rest of the spectrum resembles that of **6**, including the quasi-absence of signals for the N-bonded methyl groups. ^{89}Y solution-state NMR studies were carried out both on pure **6** and on the *rac*/*meso*-mixture. While the former displayed, in accordance with the expectation of virtually centrosymmetric, fluxional molecules (vide supra), just one sharp singlet (δ −213.4), the latter gave rise to two close-lying singlets at −212.80 and −213.01 ppm. The weaker resonance at −212.8 ppm is ascribed to the probably strictly centrosymmetric *meso*-form. The two solution-state ^{89}Y-NMR results together may be taken as one of the rare direct arguments in favour of a *di*nuclear constitution of the title complexes also in solution. Corresponding attempts to also arrive at *solution*-state ^{15}N spectra (at least of diamagnetic samples) have so far been unsuccessful.

6. Variable-temperature (VT) NMR studies

VT ^{1}H solution-state NMR studies were carried out within temperature regimes of particular relevance for rapid intramolecular $\mathbf{A}\rightleftharpoons\mathbf{B}$ rearrangements (according to Scheme 1), using $CD_3C_6D_5$ as the solvent for complexes with coalescence temperatures (T_c) above ca. 20 °C, and CD_2Cl_2 in cases of T_c values below room temperature. As an example, the result of the VT NMR study of the Yb complex **8** is depicted in Fig. 7. While here the broad *N*-methyl singlet is difficult to detect at room temperature, all ten signals to be expected for a quasi C_2- (or centrosymmetric) dimer are clearly detectable when the temperature is varied. The two low-temperature C_5H_5 singlets differ in line width, which might be indicative of more steric congestion for one of the two C_5H_5 ligands. Generally, T_c of the NMe_2 protons lies somewhat higher than for the C_5H_5 protons. The variation of T_c of the C_5H_5 and NMe_2 proton resonances, respectively, with the size and the magnetic moment of the Ln^{3+} ion is documented in Table 6. The two strongest paramagnetic metal ions Tb^{3+} and Tm^{3+} ($\mu_{eff} \sim 9.7$ and 7.6 B.M.) elevate T_c above room temperature, while T_c values below room temperature are observed e.g. for the slightly smaller, and diamagnetic,

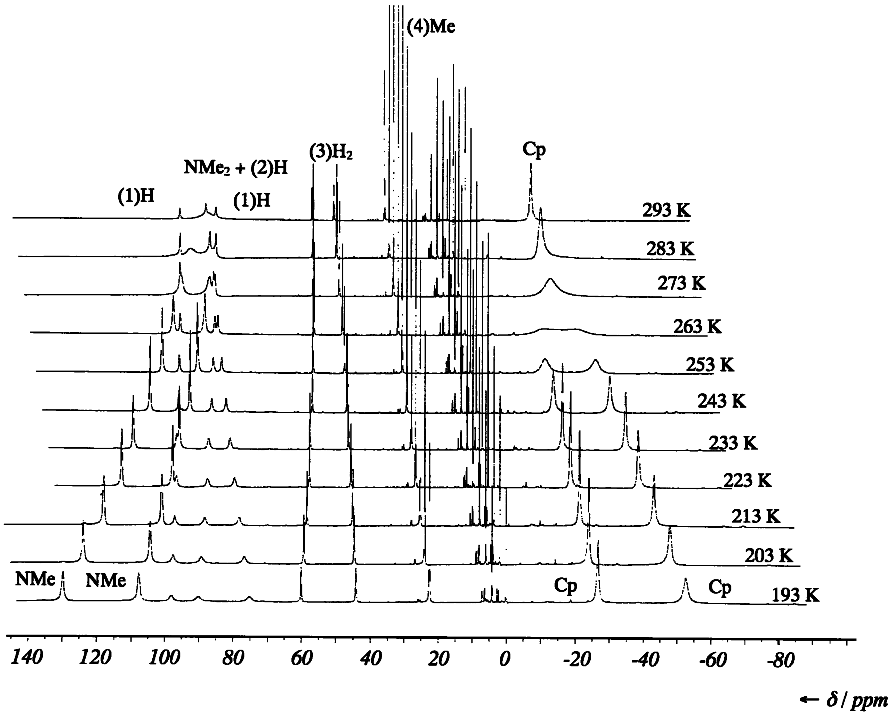

Fig. 7. Result of the VT ^{1}H-NMR study of dissolved **8** (Ln = Yb). In the notation of the signals the number in parentheses the position of the corresponding carbon atom (starting at the metal-bridging oxygen atom) signifies.

ions Y^{3+} and Lu^{3+}. Coalescence of the two NMe_2 singlets of the Tb complex could not even be reached at 95 °C. Free activation energies $\Delta G^{\#}$ were estimated [23] from the corresponding T_c and $\Delta \nu$ values (Table 6). As the separation $\Delta \nu$ of two coalescing signals increases quite rapidly with decreasing temperature when the central metal ion of a complex is paramagnetic, $\Delta \nu$ was taken throughout for the highest possible temperature (below T_c) at which two separate peaks were just observable. Interestingly, $\Delta G^{\#}$ decreases very continuously along with the ionic radius of the Ln^{3+} ion (Table 6). This correlation agrees with the expectation that the Ln–N bonds of isomer **B** (Scheme 1) would be cleaved the more readily the less space is available for the nitrogen atom within the coordination sphere of the Ln^{3+} ion. Somewhat surprisingly, $\Delta G^{\#}(NMe_2)$ consistently exceeds $\Delta G^{\#}(C_5H_5)$, and both $\Delta G^{\#}$ values of the Lu complex (**9**) are again somewhat higher than those of the Yb complex. The latter observation has been confirmed by bandshape fitting and the use of Eyring's equation [24]. Actually, the $\Delta G^{\#}$-vs-r(Ln^{3+}) correlation as expected for diamagnetic systems is not significantly perturbed by the strong paramagnetism of the Ln^{3+} ions Nd^{3+}, Tb^{3+}, Tm^{3+} and Yb^{3+}.

Equilibria involving pairs of symmetric dimers of type **B** (Scheme 1), although with two different, rapidly alternating N–Ln distances, can be ruled out as a source of the observed fluxional behaviour. In view of the pronounced reluctance of two different members of the title complexes to undergo metathetical exchange

Table 6
Characteristic properties of relevance for the fluxional behaviour of complexes **1**–**9**

Sample	Ln	Ionic radius [a] (Å)	C_5H_5 protons			$N(CH_3)_2$ protons		
			T_c (K)	$\Delta \nu$ (Hz)	$\Delta G^{\#}$ (kJ mol^{-1})	T_c (K)	$\Delta \nu$ (Hz)	$\Delta G^{\#}$ (kJ mol^{-1})
1	La	1.216	318	26	67.2	333	55	68.4
3	Nd	1.163	338	1526	60.2			
4	Sm	1.132	288	43	59.4	323	436	60.7
5	Tb	1.095	325	11 160	52.4			
6	Y	1.075	263	28	55.0	283	85	56.7
7	Tm	1.052	278	4320	46.6	315	29 963	48.1
8	Yb	1.042	268 [1]	5040	44.5	278	3334	47.2
9	Lu	1.032	217 [1]	15	46.1	248	50	49.5

[a] See Ref. [25].

(vide supra), an involvement of the mononuclear forms **C** and **D** is likewise quite improbable. Hence, the most reasonable origin of the fluxional behaviour seems to be a rapid interconversion of two formally equivalent type-**B** dimers, during which each nitrogen atom would leave its metal atom simultaneously (adopting briefly form **A**) and then anchor at the opposite metal atom. A rapid, non-concerted rupture and re-establishment of the two Ln–N bonds without crosswise back-coordination ruled out by inspecting the VT NMR spectra of one heterobinuclear system (La/Sm) [5].

7. Conclusions and outlook

Although various dinuclear rare earth complexes involving two structurally non-equivalent, but otherwise identically composed fragments have been reported [9,13,26,27], the asymmetric nature of the title compounds $[Ln(C_5H_5)_2\{\mu\text{-}OCH_2CH(Et)NMe_2\}]_2$ remains somewhat unique and difficult to understand. Thus, we have, more recently, examined also the crystal structures of three members (with Ln = La, Nd, Sm) of a closely related series of complexes [28] which had all resulted from the reaction of a distinct tris(cyclopentadienyl)lanthanoid(III) system with *N*-methyl-2-(*S*)-hydroxymethylpyrrolidine (1:1) [29]. Although, as in the title complexes, the β-carbon atoms of the metallacyclic rings represent the (primary) chiral centres (see Scheme 2), and the nitrogen atoms again carry two organic residues, all complexes of the latter family display, like the aforementioned achiral congeners [4], two almost equal Ln–N distances (i.e. for Ln = Nd: 2.812(6) and 2.816(6) Å). Interestingly, these distances match with the averaged values of the title complexes.

The praseodymium- and neodymium-containing pairs of complexes of both families display almost identical spectral patterns, reflecting excited f–f crystal field states (both in absorption and, surprisingly, also in f–f circular dichroism), which suggests that the two slightly non-equivalent alkoxide ligands generate very similar crystal fields. Thus, the non-equivalence of the two Ln–N distances in the title complexes is not reflected either by any response of the 4f electrons of the two weakly different metal centres. Although the origin of the non-superimposibility of the two metallacycles (of each title complex) is not satisfactorily evident, it is likely that by the anellation of an *N*-methylpyrrolidine ring to each of the two five-membered metallacycles, the latter might be forced to adopt one unique conformation.

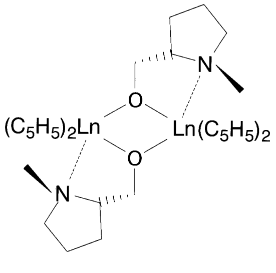

Scheme 2.

In concluding, it might be argued that in special cases of enantiomerically pure complexes of the type discussed in this study, displaying considerable steric congestion close to the chirogenic centres, the two formally equal metallacyclic rings prefer to adopt two not strictly superimposible conformations. As the {Ln–N} fragments which are most strongly affected do not belong to peripheric portions of the molecule, we are reluctant to consider crystal packing forces as mainly responsible for this observation (vide supra). At first sight, it might also seem unrealistic to assume a vague kind of ‘communication’, primarily between the two Ln–N–C fragments, but e.g. in carbohydrate chemistry (with two or more virtually equal chirogenic centres) related cases may be found [30]. The family of complexes out of which **3**–**6** have been structurally elucidated thus appears to present still rare examples fulfilling the expectation mentioned in Section 1 that by the incorporation of a chirogenic (i.e. enantiomerically pure) centre mainly the analytical tools will be improved, whereas occasionally some structural complications may be generated too. Any detailed conformational analysis should also include the corresponding *meso* form, although its isolation would be as difficult as that of a heterodinuclear derivative (vide infra). Pure meso-$[Me_2M\{\mu\text{-}OCH(Me)CH_2\text{-}Nme_2\}]_2$ was, however, obtained quite fortuitously with M = Ga, while with M = Al crystals of the pure racemate resulted [31]. Appropriate combinations of solution- and solid-state NMR investigations even of multicomponent mixtures look quite promising in the light of our successful CPMAS solid-state NMR study of **4** (vide supra). Until now, no precedent study of this degree of sophistication has been carried out in organo-rare earth chemistry.

8. Epilogue

The synthesis of bis(cyclopentadienyl)lanthanoid(III) alkoxide complexes $[LnCp_2OR]_x$ still devoid of any functionalized alkoxide ligands was first reported in 1963 [32]. The metathetical reaction of $[LnCp_2Hal]_2$ and metal alkoxides MOR (M = Li, Na, K) in THF exclusively available at that time did not afford $[Ln(C_5H_5)_2OR]_x$ systems of the ‘earlier’ lanthanoids (La–Nd), since the starting halide complexes of the largest Ln(III) ions tend to dismute too readily into $[Ln(C_5H_5)_3]$ and $[Ln(C_5H_5)Hal_2(THF)_3]$. However, since 1982, controlled alcoholysis of various

$[Ln(C_5H_5)_2R]_x$ systems (R = alkyl, hydride, cyclopentadienyl etc.) has become a strongly superior alternative [33], although quite a few well-crystallized alkoxide complexes were obtained unexpectedly during experiments of initially different goals [34]. The first successful crystal structure analysis confirming the dinuclear nature was carried out in 1986 for the already 'functionalized' complex $[Y(C_5H_4Me)_2(\mu\text{-}OCH{=}CH_2)]_2$, which was prepared both by ionic metathesis and (with ethylene as by-product) by thermolysis of $[Y(C_5H_4Me)_2CH_2SiMe_3(THF)]$ [35]. Subsequently, related enolato complexes were also obtained by 'spontaneous' dehydrogenation from saturated $[Ln(C_5H_5)_2OR]_2$ precursors in boiling THF [36]. The mechanism of this surprisingly facile reaction is still unclear. The first non-functionalized homologue containing even an 'early' lanthanoid metal, and synthesized in 1990 from $[Ce(C_5H_4CMe_3)_3]$ and $i\text{-}C_3H_7OH$, was again shown to be a symmetrical dimer [37]. Its reluctance to dismute (vide supra) contrasts notably with the instability of corresponding halide-bridged systems. With space-demanding aryloxide ligands and either *permethylated* cyclopentadienyl rings [38] or two THF ligands [39], mononuclear $LnCp'_2OR$ derivatives could also be obtained.

Crystal structures of the first oxygen- and nitrogen-functionalized derivatives, respectively, were reported in 1993 and 1998 [1,34]. Although the majority of the O- or N-functionalized alkoxide bridges contained two chirogenic centres, so far only the title complexes of the present contribution were found to display two significantly different Ln···N distances. A somewhat exceptional series of $[Ln(C_5H_5)_2(\mu\text{-}OR^N)]_2$ complexes involving the acetoximato ligand $ONCMe_2$ was already described in 1996 [40]. For Ln = Gd, two sets of Gd–O distances, two triangular metallacycles cyclic {GdON} and the chiral space group ($P2_12_12_1$) have been reported.

According to more recent, still unpublished results [5], several *hetero*dimetallic complexes containing again two (*R*)-(−)-$OCH_2CH(Et)NMe_2$ bridges could be identified by solution ^{1}H-NMR spectroscopy, although they were still intermixed with the corresponding two homodinuclear congeners. Three single crystals likely to be built up of heterodinuclear molecules (i.e. La/Sm, Pr/Sm and Nd/Sm) were subjected to X-ray crystallography. Not quite unexpectedly, the structure analyses of all three crystals revealed again two notably different Ln–N distances [41], which observation can, however, not be considered as a convincing proof of the presumed *hetero*dinuclear arrangement. An elemental analysis carried out subsequently of one of these crystals did in fact confirm the presence of almost equal amounts of La and Sm. Owing to the presence of two *chiral* alkoxide bridges and paramagnetic Sm(III), the VT ^{1}H-NMR spectra of the three-component La/Sm system actually revealed *four* different coalescence regimes of C_5H_5 resonances (two of which being attributed to the two homodinuclear complexes).

To also explore the behaviour of halogen-functionalized alkoxide ligands, some still achiral monofluoroalcohols were most recently reacted mainly with $[Nd(C_5H_5)_3]$ [22]. With 2-fluoroethanol a dinuclear complex similar to that prepared from 2-dimethylaminoethanol and $[Yb(C_5H_5)_3]$ [4] was obtained (Nd–F distances: 2.656(8) and 2.624(7) Å). While a corresponding neodymium complex with two likewise metal-anchored fluorine atoms has resulted on application of 2-fluorobenzylalcohol (Nd–F distances: 2.732(2) and 2.799(3) Å, for two independent, centrosymmetric molecules), the dinuclear yttrium 'homologue' turned out to display two non-coordinated and notably disordered fluorine atoms. One the other hand, the slightly less flexible 2-fluorophenolato ligand leads again (with Ln = Nd) to a centrosymmetric, dinuclear complex with comparatively short Nd···F contacts (2.577(5) and 2.647(5) Å for two independent molecules). A first, non-centrosymmetric congener with significant Ln···Cl contacts could, moreover, be obtained from 2-*chloro*-benzylalcohol and $[Nd(C_5H_5)_3]$ (Nd–Cl: 3.0479(17), 3.0613(15) and 3.1420(17)/3.1428(17) Å for three independent molecules).

The Nd–F distances found here tend to be slightly shorter than the averaged Nd–N distance of **3**, which may be due to the absence of space-demanding alkyl groups on the halogen atom. It seems worthwhile to expand the current exploration of dinuclear fluorine-functionalized alkoxide systems towards derivatives with a well-defined chirogenic centre in the immediate neighbourhood of the fluorine atom. For efficient comparative studies in view of the unexpected structures of **3**–**6** (vide supra), enantiomerically pure 2-fluoro-1-propanol would be most desirable, which compound is, unfortunately, commercially not available. Comparatively, few other rare earth complexes with crystallographically proved dative Ln–F interactions due to organofluorine ligands are so far reported in the literature [42].

9. Experimental

All operations were carried out under a strict N_2 atmosphere, using throughout oxygen-free, anhydrous solvents. IR spectra were obtained on a Perkin–Elmer IR 1750 instrument, and mass spectra (FAB) on a VG Analytical mass spectrometer 70-250S. Rapid Xe atoms were generated by a Xe FAB gun of Ion Teck Corp. NIR–vis absorption and corresponding circular dichroism (CD) spectra of dissolved samples (not reported here in detail) were recorded on a Carry 5 E (of Varian Inc.)

instrument and on a JASCO J200-D dichrograph, respectively, equipped with a DP-500 N data processor.

Solution NMR spectra (solvents: CD_2Cl_2 or $C_6D_5CD_3$) were obtained either on a Varian Gemini 200 instrument (200 MHz; room temperature studies of ^1H and ^{13}C only) or on a Bruker AM 360 instrument (360 MHz; room and VT studies-including the unsuccessful ^{15}N runs- and the two ^{89}Y investigations). $^1H/^1H$- and $^1H/^{13}C$-COSY correlation studies are based on measurements employing a Bruker DRX 500 instrument (500 MHz). The solid-state NMR spectra were obtained using a Varian Unityplus spectrometer operating at 14.70, 30.40 and 75.43 MHz for ^{89}Y, ^{15}N and ^{13}C, respectively. All these spectra were obtained using cross-polarisation with magic-angle spinning and using a 2 s recycle delay. The contact time was 20 ms for the ^{89}Y and ^{15}N spectra and 3 ms for the ^{13}C scans. The spectra were obtained at ambient probe temperature (ca. 22 °C) and from 300 (^{89}Y and ^{13}C) and 28 000 (^{15}N) repetitions. Sample spin-rates were between 4.5 and 4.8 kHz. Spectral referencing was made with respect to aq. $\mathit{Y}(NO_3)_3$, $CH_3\mathit{N}O_2$ or tetramethylsilane (TMS). The XRPD of **6** was obtained on a Bruker D8 Advance instrument (with Cu–K_α source and Ni filter). Data of single crystals of **3**–**6** were collected either on a Hilger & Watts Y290 four-circle diffractometer (**3**, **5**) or on a Bruker axs Smart CCD instrument (**4**, **6**), using throughout Mo–K_α radiation and the $\omega/2\Theta$ scan-technique (see also Table 1). The structures were solved either by direct methods or from Patterson maps. Refinement was based on full-matrix least-squares techniques, employing initially SHELX-93 and SHELXTL-PLUS programme sets, and subsequently the SHELXS-97 and SHELXL-97 software. Hydrogen atoms were included by use of a riding model with $d[C–H] = 96$ pm. The absolute configurations of the chiral molecules were determined by measurement of the corresponding Friedel pairs. Absorption corrections were considered either by means of the DIFABS strategy (Hilger & Watts) or by the SADABS program implemented in the Smart CCD diffractometer.

The complexes **1**, **3**, **5**, **6** and **7** (with Ln = La, Nd, Tb, Y and Tm, respectively) were prepared in yields of 70 ± 15% following essentially the details given for the earlier described homologues **2**, **4**, **8** and **9** [1]. All $[Ln(C_5H_5)_3]$ complexes had resulted from resublimation. The ligand precursors (*R*)-(−)- and (*S*)-(+)-2-(*N*-dimethylamino)butanol were synthesized starting from commercial (*R*)-(−)- and (*S*)-(+)-2-amino-1-butanol (Fluka), respectively, following Ref. [43].

1: Elemental analysis of $C_{16}H_{24}LaNO$, Calc.: C, 49.88; H, 6.28; N, 3.64. Found: C, 48.52; H, 6.35; N, 3.62%. White solid, temperature (dec.) 140 °C. ^1H-NMR (200 MHz, CD_2Cl_2, r.t.): 6.099 (s, 5H, C_5H_5), 6.037 (s, 5H, C_5H_5), 4.05 (dd, 1H, α-CH_2), 3.75 (t, 1H, α-CH_2), 2.82 (m, 1H, β-CH), 2.57 (s, 3H, N–CH_3), 2.32 (s, 3H, N–CH_3), 1.65 (m, 1H, γ-CH_2), 1.07 (m, 4H, γ-CH_2+δ-CH_3). ^{13}C-NMR (200 MHz, CD_2Cl_2, r.t.): 112.35 (C_5H_5), 112.16 (C_5H_5), 69.34 (α-C), 68.79 (β-C), 44.71 (N–CH_3), 37.93 (N–CH_3), 14.22 (γ-C), 13.00 (δ-C).

3: Elemental analysis of $C_{16}H_{24}NNdO$, Calc.: C, 49.20; H, 6.19; N, 3.59. Found: C, 48.33; H, 6.18; N, 3.42%. Light blue solid, temperature (dec.) 160 °C. ^1H-NMR (200 MHz, CD_2Cl_2, r.t.): 5.43 (bs, 5H, C_5H_5), −1.42 (bs, 5H, C_5H_5), −3.09 (bs, 1H, α-CH_2), −3.65 (s, 3H, δ-CH_3), −5.63 (bs, 1H, α-CH_2), −8.05 (s, 2H, γ-CH_2), −12.12 (bs, 1H, β-CH), −15.50 and −15.95 (each s, 3H, N–CH_3). ^{13}C-NMR (500 MHz, CD_2Cl_2, r.t.): 182.60 and 146.84 (each C_5H_5), 25.39 (β-C), 10.64 (γ-C), 8.30 (δ-C), −10.82 and −16.30 (each N–CH_3), −25.00 (α-C).

5: Elemental analysis of bulk $C_{16}H_{24}NOTb$ (the yield of exclusively crystalline **5** was too low), Calc.: C, 47.42; H, 5.97; N, 3.46. Found: C, 43.56; H, 5.89; N, 3.54%. Colourless solid, temperature (dec.) 160 °C. ^1H-NMR (200 MHz, CD_2Cl_2, r.t.): 120.18 (bs, 5H, C_5H_5), 83.08 (bs, 5H, C_5H_5), −52.69 (bs, 3H, NCH_3), −76.24 (s, 3H, δ-CH_3), −118.38 (s, 1H, γ-CH_2), −119.55 (s, 1H, γ-CH_2), −152.05 (bs, 1H, α-CH_2), −207.66 (bs, 1H, β-CH), −267.65 (bs, 1H, α-CH_2), −284.29 (bs, 3H, NCH_3). Selected MS-fragments (FAB): 745.6 (D-$C_5H_5^+$ 100%), 694.6 (D-OR^+ 15%), 588.4 (D-2OR^+ 20%), $Tb(C_5H_5)_2^+$ 11% (D = dinuclear molecule).

6: Elemental analysis of $C_{16}H_{24}NOY$, Calc.: C, 57.41; H, 7.50; N, 4.33. Found: C, 57.32; H, 7.22; N, 4.18%. Faintly brown solid, temperature (dec.) 130 °C. ^1H-NMR (360 MHz, CD_2Cl_2, r.t.): 5.99 (s, 10H, C_5H_5), 3.85 (dd, 1H, $^2J = 7.3$, $^3J = 4.7$ Hz, α-CH_2), 3.53 (t, 1H, $^{2,3}J = 11.3$ Hz, α-CH_2), 2.91 (bm, 1H, β-CH), 2.39 (s, 6H, $N(CH_3)_2$), 1.66 (bm, 1H, γ-CH_2), 1.04 (d+bm, 4H, γ-CH_2+δ-CH_3). ^{13}C-NMR (200 MHz, CD_2Cl_2, r.t.): 109.74 (C_5H_5), 68.51 (α-C), 67.76 (β-C), 41.78 ($N(CH_3)_2$), 14.53 (γ-C), 12.99 (δ-C). The mixture of racemic and *meso*-**6** was synthesized from $[Y(C_5H_5)_3]$ and racemic 2-dimethylaminobutanol. Elemental analysis, Found: C, 57.32; H, 7.22; N, 4.18%. ^1H-NMR (360 MHz, CD_2Cl_2, r.t.): 6.01 (s, 10H, C_5H_5 *meso*), 6.00 (s, 10H, C_5H_5 *rac*), 3.97 (dd, 1H, $^2J = 7.3$, $^3J = 4.7$ Hz, α-CH_2 *meso*), 3.87 (dd, 1H, $^2J = 7.3$, $^3J = 4.7$ Hz, α-CH_2 *rac*), 3.54 (t, 1H, $^{2,3}J = 11.3$ Hz, α-CH_2 *rac*), 3.49 (t, 1H, $^{2,3}J = 11.3$ Hz, α-CH_2 *meso*), 2.92 (bm, 2H, β-CH *rac*+*meso*), 2.39 (s, 12H, $N(CH_3)_2$ *rac*+*meso*), 1.66 (bm, 2H, γ-CH_2 *rac*+*meso*), 1.04 (s+bm, 8H, γ-CH_2 *rac*+*meso* and δ-CH_3 *rac*+*meso*). ^{13}C-NMR (200 MHz, CD_2Cl_2, r.t.): 109.96 (C_5H_5 *meso*), 109.70 (C_5H_5 *rac*), 69.21 (α-C *meso*), 68.54 (α-C *rac*), 67.78 (β-C *rac*), 67.72 (β-C *meso*), 14.57 (γ-C, *rac*+*meso*), 13.04 (δ-C *rac*+*meso*). Approximate *rac*/*meso* ratio: 3/2.

7: Elemental analysis of bulk $C_{16}H_{24}NOTm$ (the yield of exclusively crystalline **7** was too low), Calc.: C, 46.27; H, 5.82; N, 3.37. Found: C, 42.27; H, 5.59; N, 3.71%.

Yellowish solid, temperature (dec.) 150 °C. ^{1}H-NMR (200 MHz, CD_2Cl_2, r.t.): 162.64 (s, 1H, α-CH_2), 144.92 (s, 1H, α-CH_2), 130.01 (bs, 3H, NCH_3), 116.63 (s, 1H, β-CH), 70.23 (s, 1H, γ-CH_2), 65.59 (s, 1H, γ-CH_2), 44.49 (s, 3H, δ-CH_3), 26.62 (bs, 3H, NCH_3), −22.73 (bs, 10H, C_5H_5). Selected MS-fragments (FAB): 765.6 (D-$C_5H_5^+$, 100%), 714.5 (D-OR$^+$, 15%), 638.4 (D-2OR$^+$, 17%), 939.7 (unknown, 30%).

10. Supplementary material

Crystallographic data have been deposited with the Cambridge Crystallographic Data Centre, CCDC nos. 192612, 192613, 192614 and 192611 for compounds **3**, **4**, **5** (at two temperatures) and **6**, respectively. Copies of this information may be obtained free of charge on application to The Director, CCDC, 12 Union Road, Cambridge CB2 1EZ, UK (fax: int. code +44-1223-336-033; e-mail: deposit@ccdc.cam.ac.uk or www: http://www.ccdc.cam.ac.uk).

Acknowledgements

We thank Professor U. Behrens (Hamburg) for numerous essential hints regarding the crystal structure analyses, S. Samba for technical assistance and the U.K. EPSRC for access to the National Solid-state NMR Research Service based at Durham.

References

[1] A. Steudel, E. Siebel, R.D. Fischer, G. Paolucci, V. Lucchini, J. Organomet. Chem. 556 (1998) 229.

[2] Related mononuclear systems involving Me_2M fragments (M = Al, Ga) instead of Cp'_2Ln have structurally been characterized: (a) R. Kumar, M.L. Sierra, J.P. Oliver, Organometallics 13 (1994) 4285;
(b) E. Hecht, T. Gelbrich, S. Wernik, R. Weimann, K.-H. Thiele, J. Sieler, H. Schumann, Z. Anorg. Allg. Chem. 624 (1998) 1061;
(c) J. Lewinski, J. Zachara, T. Kopec, K.B. Starowieyski, J. Lipkowski, I. Justyniak, E. Kolodziejczyk, Eur. J. Inorg. Chem. (2001) 1123.

[3] A. Steudel, J. Stehr, E. Siebel, R.D. Fischer, J. Organomet. Chem. 570 (1998) 89.

[4] T. Hahn, Doctoral Dissertation, Universität Leipzig, Germany, 2001; T. Hahn, P. Junk, E. Hey-Hawkins, to be published (Polyhedron).

[5] K. Schierwater, H. Hanika-Heidl, R.D. Fischer, to be published.

[6] (a) R. Anwander, W.A. Herrmann, F.C. Munck, W. Scherer, J. Organomet. Chem. 462 (1993) 163;
(b) C. Qian, B. Wang, D. Deng, G. Wu, P. Zheng, J. Organomet. Chem. 427 (1992) C29.

[7] W.A. Herrmann, R. Anwander, F.C. Munck, W. Scherer, Chem. Ber. 126 (1993) 331.

[8] H. Schumann, J.A. Meese-Marktscheffel, A. Sietrich, F.H. Görlitz, J. Organomet. Chem. 430 (1992) 299.

[9] A. Steudel, J. Stehr, E. Siebel, R.D. Fischer, J. Organomet. Chem. 510 (1996) 197.

[10] H. Schulz, H. Reddmann, H.-D. Amberger, B. Kanellakopulos, C. Apostolidis, J. Rebizant, N.M. Edelstein, J. Organomet. Chem 622 (2001) 19.

[11] W.A. Herrmann, R. Anwander, M. Kleine, W. Scherer, Chem. Ber. 125 (1992) 1971.

[12] H. Schumann, S. Wernik, B.C. Wassermann, F. Girgsdies, J. Organomet. Chem. 621 (2001) 254.

[13] Q. Liu, J. Huang, Y. Qian, A.S.C. Chan, Polyhedron 18 (1999) 2345.

[14] Z.-Z. Wu, Z.-E. Huang, R.-F. Cai, Z. Xu, X.-Z. You, X.-Y. Huang, Polyhedron 15 (1996) 13.

[15] W.A. Herrmann, R. Anwander, M. Kleine, K. Öfele, J. Riebe, W. Scherer, Chem. Ber. 125 (1992) 2391.

[16] H. Schumann, F. Erbstein, R. Weimann, J. Demtschuk, J. Organomet. Chem. 536 (1997) 541.

[17] W.J. Evans, J.H. Meadows, A.J. Kostka, G. Closs, Organometallics 4 (1985) 324.

[18] G.W. Rabe, A. Sebald, Solid State Nucl. Magn. Reson. 6 (1996) 197.

[19] P.L. Watson, J. Am. Chem. Soc. 105 (1983) 6491.

[20] W.J. Evans, J.H. Meadows, W.E. Hunter, J.L. Atwood, J. Am. Chem. Soc. 106 (1984) 1291.

[21] See: C.A. McDowell, in: D.M. Grant, R.K. Harris (eds.-in-chief), Encyclopedia of NMR, vol. 5, 1996, p. 2901.

[22] K. Schierwater, R.D. Fischer, unpublished results.

[23] See: H. Friebolin, Basic One- and Two-Dimensional NMR Spectroscopy, Wiley-VCH, Weinheim, Germany, 1998, p. 309; H. Günther, NMR-Spektroskopie, G. Thieme Publ., Stuttgart, Germany, 1992, p. 310.

[24] V. Lucchini, University of Venice, Italy, personal communication.

[25] R.D. Shannon, Acta Crystallogr. Sect. A 32 (1976) 751.

[26] Q. Liu, M. Ding, Y. Lin, Y. Xing, Polyhedron 17 (1998) 555.

[27] R. Anwander, F. Munck, T. Priermeier, W. Scherer, O. Runte, W.A. Herrmann, Inorg. Chem. 36 (1997) 3545.

[28] Details of the crystal structure determination have been deposited as Special Publications with the Cambridge Crystallographic Data Centre under the CSD numbers: 196709 (Nd) and 196710 (La).

[29] K. Schierwater, R.D. Fischer, unpublished results. The corresponding praseodymium complex was first described by J. Stehr, Doctoral Dissertation, Universität Hamburg, Germany, 1993, p. 105.

[30] See: S.J. Angyal, J.K. Saunders, C.T. Grainger, R. Le Fur, P.G. Williams, Carbohydr. Res. 150 (1986) 7; J. Kopf, M. Morf, B. Zimmer, P. Köll, Carbohydr. Res. 218 (1991) 9.

[31] K.-H. Thiele, E. Hecht, T. Gelbrich, U. Dümichen, J. Organomet. Chem. 540 (1997) 89.

[32] R.E. Maginn, S. Manastyrskyj, M. Dubeck, J. Am. Chem. Soc. 85 (1963) 672.

[33] See e.g. H. Schumann, W. Genthe, N. Bruncks, J. Pickardt, Organometallics 1 (1982) 1194; P.L. Watson, J. Chem. Soc. Chem. Commun. (1983) 276; W.J. Evans, J.H. Meadows, W.E. Hunter, J.L. Atwood, J. Am. Chem. Soc. 106 (1984) 1291; for a complete list of structure analyses reported until 1996 see: Z.-Z. Wu, Z.-E. Huang, R.-F. Cai, Z. Xu, X.-Z. You, X.-Y. Huang, Polyhedron 15 (1996) 13.

[34] G. Massarweh, R.D. Fischer, J. Organomet. Chem. 444 (1993) 67.

[35] W.J. Evans, R. Dominguez, T.P. Hanusa, Organometallics 5 (1986) 1291.

[36] Z. Wu, Z. Xu, X. You, X. Zhou, Y. Xing, Z. Jin, J. Chem. Soc. Chem. Commun. (1993) 1494; Z. Wu, Z. Xu, X. You, X. Zhou, X. Huang, J. Organomet. Chem. 483 (1994) 107.

[37] S.D. Stults, R.A. Anderson, A. Zalkin, Organometallics 9 (1990) 1623.

[38] W.J. Evans, T.P. Hanusa, K.R. Levan, Inorg. Chim. Acta 110 (1985) 191.

[39] G.B. Deacon, S. Nickel, E.R.T. Tiekink, J. Organomet. Chem. 409 (1991) C1.

[40] Z.-Z. Wu, D.-M. Fan, Z.-E. Huang, R.-F. Cai, Polyhedron 15 (1996) 127.

[41] Details of the crystal structure determination have been deposited as Special Publications with the Cambridge Crystallographic Data Centre under the CSD numbers 199221 (La/Sm), 199222 (Pr/Sm) and 199223 (Nd/Sm).

[42] J.H. Melman, C. Rohde, T.J. Emge, J.G. Brennan, Inorg. Chem. 41 (2002) 28.

[43] A. Kaluszner, A.B. Galun, J. Org. Chem. 26 (1961) 3536.